Optimization of bending strength for cold roll formed steel channel sections using Finite Element modelling

Sangar Jamal Qadir[1]

Abstract

In this study, the buckling and ultimate strengths of cold rolled channel sections with intermediate stiffeners were studied using numerical modelling. In order to improve the section strength, various alternative sections of varying intermediate stiffeners were developed and searched for the maximum ultimate strength. The section flexural strength was optimized through a practical approach that combines finite element modelling and optimization using design of experiments (DOE) and response surface methodology. In this approach, a nonlinear finite element model was first developed for a referenced channel section subjected to four-point bending tests and this reference section was then parameterized in terms of geometric dimensions and material properties using the DOE technique. In the next step, a response surface was used to determine the influences of the stiffener's properties on the section distortional buckling and ultimate strength including its location, shape, size and material properties by the cold work at the section corners and stiffener bends. Response surface design optimization was then used to determine the geometric dimensions and material properties of novel channel sections. The new optimized channel sections were then applied loading up to failure to obtain ultimate flexural strengths and the results were compared to those of the reference channel section. It was found that sections with maximum ultimate strength in distortional buckling could be obtained with both the stiffeners' position, shape and size, and the cold work influence. The cold work influence was found most significant in the novel channel sections. An optimal shape for the channel section with maximum ultimate strength in distortional buckling could be obtained without increasing the amount of the material used.

Keywords

Optimization; cold rolled steel; distortional buckling; ultimate strength; Finite Element modelling; Design Of Experiments; cold work effect

1. General

Cold-formed steel (CFS) structural elements are widely used in various applications in building construction as secondary members, such as framing members, purlin, lintels, side rail, gable systems etc. and also as primary members in primary structure in low to mid-rise buildings. CFS members are often produced by cold rolled forming or press braking processes, that are found to be more economical and efficient compared to hot-rolled steel structure counterparts, where they can be available in a choice of systems to suit virtually any requirement in terms of span, load, and complexity. The most economic method of manufacturing cold-formed sections is generally the cold rolled forming process. In this method, most advanced profile systems for almost every cross-section type have been produced and made construction faster and easier. This versatility on the manufacturing side has required the structural engineers seeking for optimal design solutions that minimize the initial steel strip of the cross-section to a minimum while maintaining the structural performance, hence reducing the major financial outlay in the process which is the material cost.

Previous studies on the Optimization of CFS sections have primarily limited to use analytical formulas or the methods available in the Codes and Specifications such as AISI-S100 Specification [1], BS5950 [2], and Eurocode 3 (EC3) [3] (i.e. the Effective Width Method (EWM) and the Direct Strength Method (DSM)) to calculate the elastic buckling, compression and flexural strength of the structural members.

Analytical formulas were developed to calculate local and global buckling strengths of CFS cross-section beams such as a mono-symmetrical open cross-sections and cosinusoidally corrugated flanges, I-sections with mono and anti-symmetrical I-shapes, and channel beams with closed hollow flanges [4-7].

[1] PhD, Department of Civil Engineering, University of Sulaimani, sangar.qadir@univsul.ed.iq

In these studies, the flexural strengths were Optimized in a process to achieve practical solutions in a design space constrained by geometric conditions. The results indicated that the global and local buckling strengths of the Optimized sections could be enhanced compared to the standard plain and lipped channel sections.

Previous researchers used the analytical equations only to maximize the second moment of area and minimize the

cross-sectional area of CFS beams [8, 9]. The results provided an optimal shape obtained from arbitrary selected cross-sections. Other researchers performed global Optimization of CFS channel beams using the trust-region method and the results of Optimized sections were compared with those obtained from the application of BS5950 [2] and EC3 [3]. It was found that these two design guidelines provided almost the same Optimized section area. The EWM in AISI specification [1] was used to develop an optimal design of predefined orthodox CFS cross-sections including hat, I-, and Zed- beams [10], lipped channel beams [11], hat-shape beams and channel columns with and without the edge stiffeners [12]. Thus, the study results proposed optimal design curves for various load levels.

The Effective width/Effective thickness methods available in EC3 were used to calculate local, distortional, and global buckling strengths of compression [13] and flexural [14, 15] structural members. The strength capacities of different cross-sectional prototypes were Optimized using Genetic Algorithms and Particle Swarm Optimization. The researchers also evaluated the adequacy of EC3 in predicting the changes in strength capacity as a result of increasing/decreasing geometric parameters using detailed nonlinear FE modelling. While this led to some innovative new geometries, the only optimal design sections were verified by using FE models accounting for material and geometric nonlinearities and imperfections; hence casting some doubt on the Optimization approaches.

All these design methods available in the design guidelines [1-3] use the Effective Width Method for strength determination. This method is feasible for rather conventional sections for which a distinction between web, flanges and lips can be made and which fall within the dimensional limits of the design standard. It becomes problematic, however, when the aim is to generate novel, previously undiscovered shapes in a free-shape optimization, as the conventional standards are typically not applicable.

The Finite Strip Method (FSM) and the DSM were used as an alternative in some of the recent optimization studies of CFS structural members [16-26]. The DSM only needs the elastic critical local, distortional, and global buckling stresses calculated in order to predict the strength capacity and can therefore, in principle, be applied to any shape. The elastic buckling stresses can thereby be obtained from a Finite Strip (FSM) analysis.

The method employed in the majority of these studies was solely restricted to columns with unconstrained (where the Optimizations are free to obtain any cross-sectional shapes results in impractical irregular or curved shapes which are expensive or impossible to manufacture) [16-20] and constrained (where the sections can be practicably manufactured and assembled onsite) [21-23]. Other very few limited Optimization studies of CFS beam and beam-column have also been found [24-26] where the optimization was carried out using the DSM. This method, however, does incur some shortcomings. The statistical correlation between a cross-sectional slenderness parameter and the ultimate strength capacity was used to develop the DSM equations. This may exhibit a significant coefficient of variation and make the DSM predictions significantly cross-sectional dependent, resulted in providing more accurate prediction for certain cross-sections than for others. The DSM ignores distortional-global or local-distortional interactions [27]. This can be significantly problematic as reported Optimization results may not be correctly predicted.

Only two Optimization studies have been found [28, 29], focusing on maximizing energy dissipation in a cantilever beam under monotonic and cyclic loads, where the Optimization was performed using the general purpose finite element program accounting for geometric and material non-linearity and initial imperfections (GMNIA). A Simulated Annealing algorithm was combined with detailed nonlinear FE models to obtain hot-rolled H-beams with optimal flange shapes that the energy dissipation capacity was significantly improved [28]. A Particle Swarm Optimization (PSO) algorithms was combined with detailed FE models to perform size Optimization of 15 CFS cross-sectional prototypes [29]. The Optimized cross-sectional shapes were dissipated up to 60% more energy compared to commercially available lipped channel. While these two studies could be considered as an essential step toward a robust and an efficient Optimization procedure, some shortcomings were reported and could be observed from the studies. They were reported to be substantially computationally expensive and they were performed on the high-performance computing system. The FE models were not validated against experimental testing before using them for the Optimization studies. The later study [29] validated against four-point beam bending tests, whereas it was used for the Optimization of a cantilever beam. While the later study [29] focused on CFS members, the effect of clod work in the corners and stiffeners' bends induced from the manufacturing process was ignored.

The focus of the research presented in this paper was to develop a new practical approach to Optimize CFS channel sections with longitudinal intermediate stiffeners in the flanges and web under bending while considering both the stiffeners' geometry and cold work influences on the buckling and ultimate bending strength of channel sections. A Finite Element model was first developed to replicate four-point bending tests of an industrial channel section and the results were validated against the experimental data. The channel section was then parameterized in terms of geometric dimensions and material properties using the

DOE technique. In this approach, the dimensions, the initial imperfections, and the cold work effect induced from cold roll forming of the channel were defined as parameters in the Finite Element modelling; in the design of experiments, these parameters were assigned a range of values to determine sampling points. The sampling points obtained from DOE method was used to construct Response Surface (RS) which combined DOE methods and mathematical statistics, continuously testing the specified points until the relationship between parameters was solved. The kriging response surface was used to determine the influences of the stiffener's properties on the section distortional buckling and flexural strength including its location, shape, size, and material properties by the cold work at the section corners and stiffener bends. Response surface Optimization was finally used to determine the geometric dimensions and material properties that provided the optimal design of the channel sections.

2. Finite Element modelling

Qadir et al. [30] presented FE models capable of simulating the buckling and ultimate bending strength of cold rolled steel beam sections. Their FE models, which were developed in ANSYS (ANSYS, Inc.) and verified against earlier experimental testing [31], were used to calculate buckling, developed stresses and ultimate bending strength in this paper.

All the beams had a total length of 2920 mm, a span of 2691 mm, and a load center of 897 mm (i.e. four-point bending). Lateral bracings were provided to prevent lateral torsional buckling in all FE models. The elastic modulus E of 205 GPa and material yield strength f_y of 519.4 MPa were assigned to the flat part of all beam sections and enhanced yield strength at the corners and stiffeners bends of the sections. Two methods were used to generate the shape of initial geometric imperfections namely Finite Element method using ANSYS and Finite Strip Method using CUFSM as well as the 75% of CDF magnitude corresponding to 1.55t [32] was taken for the amplitude of initial imperfections. See [30] for full details on FE modelling.

3. Optimization Method

Figure 1 (a) shows a cross section and general dimensions for the channel section beam which was the industrial UltraBEAM^{TM2} section (Hadley Industries plc.). The study goal was to find optimal design of the web and flange stiffeners' positions, shapes, sizes, and enhanced material properties at corners and stiffeners' bends, which enhance the section's buckling and ultimate bending strength, leading to an optimal design of the channel section. The FE model developed and validated in [30] was utilized for the Optimization study. The channel section together with its bending setup used in the experimental testing in [31] were defined as "reference section" and shown in Figure 1 (a). The section height h and thickness t were fixed in the Optimization study.

The section without flange stiffeners is shown in Figure 1 (b), in which all dimension parameters are also shown and the section with flange stiffeners is shown in Figure 1 (c). The values for h and t were taken of the reference section as 170.10 mm and 1.60 mm, respectively. p_1 and p_2 are the position of the web stiffener from the web-flange junction, p_3 is the position of the peak of the web stiffener in horizontal direction from the web-flange junction, p_4 is the width of the edge stiffener, p_5 is the radius of the section corners and it was assumed that they had the same radius, p_6 and p_7 are the angle of rotation of the web stiffener, p_8 is the flange width, p_{15} is the position of the flange stiffener away from web flange junction, and p_{16} and p_{17} are the size of the flange stiffener (assuming the flange stiffener had a circular shape).

For the channel section shown in Figure 1 (b) and (c), a total of 270 combinations between p_1, p_2, p_3, p_4, p_5, p_6, and p_7 were considered with lower bound of 1.00 mm and upper bound of 40.53 mm for p_1 and p_2, lower bound of 5.61 mm and upper bound of 23.61 mm for p_3, lower bound of 2.90 mm and upper bound of 7.50 mm for p_5, lower bound of 0.00 degree and upper bound of 20.00 degree for p_6 and lower bound of 340.00 degree and upper bound of 360.00 degree (equivalent of 0.00 degree) for p_7. The reference section had $p_1 = p_2$ = 10.53 mm, p_3 = 13.61 mm, p_4 = 12.35 mm, p_5 = 2.90 mm, p_6 = 0.00 degree and p_7 = 360.00 degree = 0.00 degree. Hence, the buckling, flexural strength capacity with the cold work effect for each change were obtained and compared to evaluate the effect of these changes.

The total length of the channel cross section was kept unchanged for the Optimization target, that was "obtaining maximum strength of the section while maintaining the same weight". Changes in parameters relating to the stiffeners' shapes, sizes, positions while considering enhanced material properties at corners and bends by the cold work effect resulted in new channel sections. The material properties at the flat regions, corners and at the stiffeners' bends were assumed to be the same in these new sections. In summary, the reference section had an initial imperfection of 1.55t, an elastic modulus E of 205 GPa, a Poisson's ratio ν of 0.3 and the stress-strain data determined in [30] for the flat, corners and stiffener's bends.

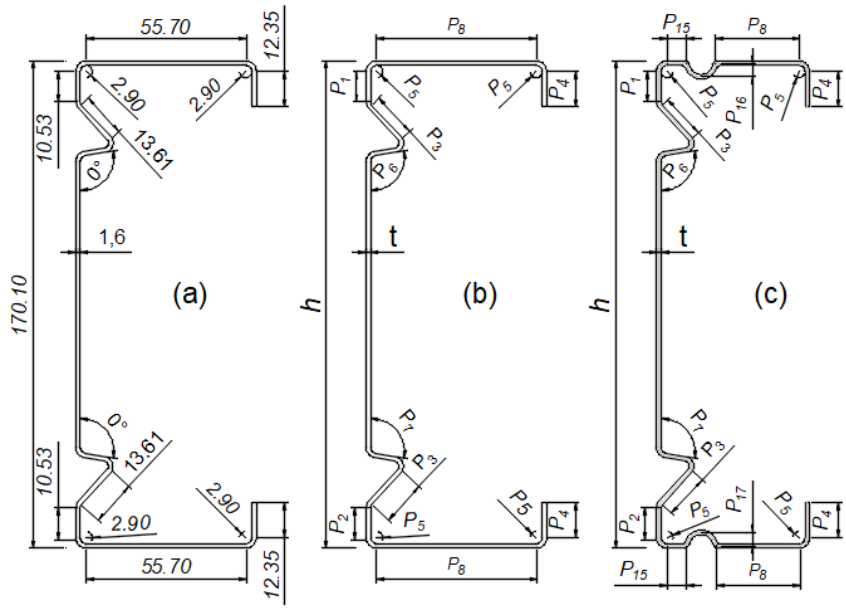

Figure 1: Dimension parameters in (mm) and definition of design variables of the channel cross section (a) reference section, (b) without flange stiffeners, and (c) with flange stiffeners

3.1 Calculation flow chart for FE modelling and Optimization

Figure 2 shows calculation procedures performed in this study. First, the three dimensional of the steel channel section beam was built, allowing for the ten parameters to be parameterized (the positions (p_1 and p_2), size and shape (p_3, $p_6$and p_7) of web stiffeners, the size of edge stiffeners (p_4) and section corners (p_5), the positions of flange stiffener (p_{15}), and the size of flange stiffener (p_{16}-p_{17})). Next, the linear buckling analysis was carried out in the Static Structural analysis at the initial dimensions (i.e. the reference section dimensions) before conducting eigenvalue buckling analysis. Because eigenvalue analysis was based on the Static Structural solution, a Static Structural analysis was a prerequisite. Then, the nonlinear buckling analysis was performed including geometry and material nonlinearity, initial imperfections, and the cold work effect at section corners and stiffeners' bends. This linked setup allowed the three analysis systems to share resources such as engineering data, geometry, and boundary condition type definitions made in Static Structural analysis. Finally, the response surfaces were calculated, and the best design candidates were selected using a multi-objective genetic algorithm.

3.1.1 Design OF Experiment

Design Of Experiment (DOE) is a technique used to efficiently find the location of sampling points. ANSYS provides several DOE types such as Central Composite Design, Optimal Space-Filling Design, Box-Behnken Design, Custom, Custom + Sampling, Sparse Grid Initialization, Latin Hypercube Sampling Design, and External Design of Experiments.

All the DOE types have common characteristics, which try to locate the sampling points such that the space of random input parameters is explored in the most efficient way and obtain the required information with a minimum design points. Determining efficient locations of sampling points could reduce the required number of design points and increase the accuracy of response surface as well.

In this study, the Custom DOE type was selected to determine the location of sampling points. The main reason was due to complex geometry of the channel sections. The sections had to be kept symmetry for the practical purpose and to use the same amount of material in all the cases. It was not possible to fulfil these conditions when using other methods. Using the Custom DOE, design points were manually added to the design points table by introducing the parameters and the desired levels into which they required to be divided. Thus, the Custom DOE type was the right choice to fill sampling space efficiently in this study.

In this approach, the dimensions of the channel section were defined as geometric parameters in the Finite Element modelling; in the design of experiments, these parameters were assigned a range of values to determine parameter values that achieved the target Optimized performance. This was performed under different level of applied loads, searching for the sections that could withstand maximum loads before they failed. In the DOE method, the cross-sectional shapes that resisted maximum applied load (best design candidate) were selected. This means that the

Optimized sections were chosen from a certain number of alternative solutions, the number of which decided the accuracy. Due to substantially more computational time, this method provided limited design candidates. The so-called best design candidate was not the Optimization in its true meaning.

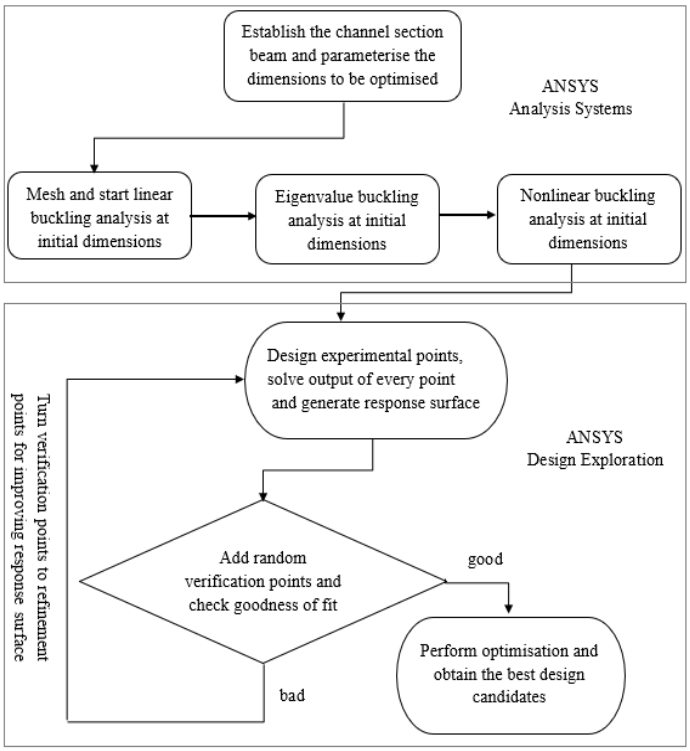

Figure 2: FE modelling and optimization flow chart.

In principle, the DOE method was utilized to find the location of sampling points in a way that the space of random input parameters (p_1-p_7) and (p_{15}-p_{17}) was explored in the most efficient way and that the target Optimized performance (p_{13} and p_{14}) could be calculated with the minimum number of sampling points. In this study, the target Optimized performances (also called target objectives) were maximizing buckling loads (p_{13}) and minimizing the maximum flexural developed stresses (p_{14}) under constant applied load. The sampling points obtained from DOE method could be used to construct Response Surface (RS) which combined DOE methods and mathematical statistics, continuously testing the specified points until the relationship between parameters was solved. This established the RS and constructed the approximation of target parameters in a global design space. This method involved simple calculations and fit a complex response relationship, hence overcoming the problems of limited design points used in the DOE methods.

3.1.2 Response surface

Response surfaces (RS) can be defined as functions in which the output parameters are described in terms of the input parameters. RS generate an approximation of the response variable over the design space using the results of a DOE. The main idea to use RS is that they quickly provide the approximated values of the output parameters throughout the design space without having to perform a complete solution. This could estimate the set of input parameters and yield an optimal response. Since the RS is an analytical function, the Optimization process is quite quick and generally does not require additional simulations or experiments to be conducted.

ANSY supports different RS techniques such as Genetic Aggregation, Full 2nd-Order Polynomials, Kriging, Non-Parametric Regression, Neural Network, and Sparse Grid. Kriging method was used in this study and briefly explained here.

Kriging is an accurate multidimensional interpolation combining a polynomial model, which provides a “global” model of the design space and local deviation. This enables kriging model to interpolate the DOE points. It is a meta-modeling algorithm that provides an improved response quality and fits higher order variations of the output parameter. It is efficient in numerous cases particularly when the output response is highly nonlinear. It can be expressed as

$$Y_{(X)} = f_{(x)} + Z_{(x)} \quad (1)$$

Where $Y_{(X)}$ is the unknown function of interest, $f_{(x)}$ is a polynomial function of (x), and $Z_{(x)}$ is the realization of a normally distributed Gaussian random process with mean zero, variance σ^2, and non-zero covariance. The $f_{(x)}$ term is similar to the polynomial model in a response surface and provides a "global" model of the design space.

While $f_{(x)}$ "globally" approximates the design space, $Z_{(x)}$ creates "localized" deviations so that the Kriging model interpolates the (N) sample data points. The covariance matrix of $Z_{(x)}$ is given by:

$$Cov[Z(x^i), Z(x^j)] = \sigma^2 R([r(x^i, x^j)]) \quad (2)$$

Where R is the correlation matrix and $r(x^i, x^j)$ is the spatial correlation of the function between any two of the (N) sample points. The correlation function $r(x^i, x^j)$ is a Gaussian correlation function:

$$r(x^i, x^j) = \exp\left(-\sum_{k=1}^{M} \theta_k \left|x_k^i - x_k^j\right|^2\right) \quad (3)$$

The θ_k is the unknown parameters used to fit the model, (M) is the number of design variables, and x_k^i and x_k^i are the k^{th} components of sample points x^i and x^j.

The effectiveness of the RS is generally verified by Goodness of Fit metrics and Verification Points in ANSYS. Kriging fits the RS through all design points, which cannot be verified by only Goodness of Fit metrics. Thus, a randomly generated test points (verification points) was used with Goodness of Fit to verify the effectiveness of the RS in this study.

Then, the RS was used to plot the response (output) vs. each of the input parameters (i.e. single and double) and to calculate the sensitivities. This could allow the user to select, for Optimization, only the parameters to which the outputs (buckling load and developed stresses) were sensitive. This could minimize the need for experimentation to only limited input parameters. All the input parameters, however, were found to be sensitive to the outputs in this study. Hence, all the input parameters were included to conduct Optimization.

Within RSO, Optimization was performed by using the RS rather than actual evaluation of the response via finite element modelling (FEM). This resulted in significant saving of computational time, but the result was approximate since the RS approximated the actual output function.

3.1.3 Optimization

Once the response surfaces were generated and the correlations between input and output parameters were well understood, the final step was to Optimize the channel sections design. In this study, the Response Surface Optimization (RSO) was used to determine the most suitable candidates and ultimately identify the optimal design of the channel sections.

The RSO was based on a DOE and obtained its information from the RS. The results of RSO were significantly dependent on the RS quality. The optimal results, although it was just an approximation since the algorithms to be used for the RS evaluations rather than actual solution from new simulations, could be obtained without further computational time. It is worth mentioning that the significant computational time was to be spent in the DOE step.

Many various Optimization methods are available for RSO in ANSYS software such as Screening, Multi-Objective Genetic Algorithm (MOGA), Nonlinear Programming by quadratic Lagrangian (NLPQL), and Mixed-Integer Sequential Quadratic Programming (MISQP).

Only screening and MOGA are multi-objective methods. Screening uses a quasi-random number generator based on Hammersley algorithm, which is a direct sampling method. It is typically used to determine a first set of candidate points for a preliminary design. If refinements are needed, these points are then used as starting point for other Optimization methods. On the other hand, MOGA is an iterative method that uses a genetic algorithm to optimize problems with continuous input parameters and to create the initial samples. Using cross-over and mutation for the next populations, MOGA iteratively searches for the feasible points for generating Pareto front. There is rarely a feasible solution to minimize or maximize all objective functions simultaneously. In this situation, there is typically a group of solutions called Pareto optimal solutions. They are solutions that cannot be improved in any of the objectives without deteriorating at least one other. There is usually an infinite number of Pareto optimal solutions, and they are usually referred to as the Pareto front.

There were two main objectives in this study namely maximizing buckling loads and minimizing the maximum developed stresses. Therefore, the MOGA method was selected to perform Optimization.

4. Results and discussion

This section presents the results of investigating the influence of both the web and flange intermediate stiffeners' positions, shapes, sizes and cold work effect at corners and stiffeners' bends on the section buckling and flexural strengths. DOEs were performed to determine the optimal configuration of channel sections, 172 simulations performed for the channel sections without flange stiffeners and 189 simulations performed for the channel sections with flange stiffeners. Once the DOEs had completed, the Kriging algorithm was used to construct the response surface without refinement. Then, 30 verification points were simulated and used, along with the DOE points, to check the quality of DOE predictions.

Once the optimal DOE was selected, an analysis of the influences of both the web and flange intermediate stiffeners' positions, shapes, sizes and cold work effect at corners and stiffeners' bends on the section buckling and flexural strengths was performed to observe the effect of parameters. Finally, Response Surface Optimization was performed using the MOGA method to determine the design candidates that Optimize the buckling and flexural strength of the channel sections.

4.1 Design of experiment quality metrics

Figure 3 shows the graph of the comparison between the value of the buckling (Total Deformation Load Multiplier p_{13})

and flexural strength (Equivalent Stress Maximum p_{14}) of design points as well as the predicted value from response surface. Verification points simulated to check the quality of DOE predictions are also shown in the graph. From the graph, it can be seen that a generated response surface was relatively accurate to achieve good-enough quality criteria. Hence, the response surface could be used for future analysis and Optimization.

4.2 Response surface results

The buckling (Total Deformation Load Multiplier p_{13}) and flexural strength (Equivalent Stress Maximum p_{14}) results obtained from changing different parameters are presented in this section. The parameters investigated were the influences of both the web and flange intermediate stiffeners' positions, shapes, sizes and cold work effect at corners and stiffeners' bends. The results obtained from performing Eigenvalue buckling analysis under a unite applied load and performing non-linear buckling analysis under applied load of 11.50 kN. The sections developed less flexural strength under this applied load have often high ultimate flexural strength capacity compared with those developed high flexural strength when they loaded up to failure.

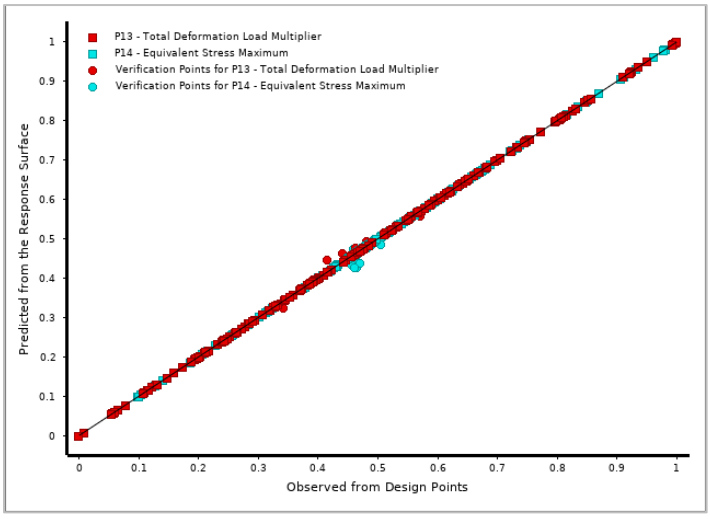

Figure 3: Normalized charts of the predicted vs observed values of section buckling and strength for DOE configuration. Square points are the DOE points and circular ones are the verification points. The black line shows the line in which the points could have a predicted value from response surface equal to the observed one in the design points.

Figure 4 is the response surfaces of the single parameter in initial values of the channel section with flange stiffeners. It was seen that buckling decreasing gradually to its lowest point and developed stresses increasing gradually to its highest point around $p_1 = 40\ mm$. Increasing (p_1) was the same as moving down the stiffeners towards the center of the cross section. The reduction in the buckling and increasing in the developed stresses were due to the fact that when increasing (p_1), it generated new cross sections with a reduction in the section modulus and an increase in the buckling slenderness. In combination, the buckling considerably reduced by 4% and the developed stresses considerably increased by 6% when increasing (p_1) due to a product of the increasing effect by the buckling slenderness λ_d and the decreasing effect of the sectional modulus S_{xx}.

Local sensitivity represents the change of the outputs based on the change of inputs independently. A positive value of the sensitivity means that as the input parameter increases, the output increases as well; and a negative value means the opposite. Figure 5 shows the sensitivities of the main output parameters including the buckling (p_{13}) and the flexural strength (p_{14}) that were based on the input parameters, namely, the web stiffener's positions from the web-flange junction (p_1 and p_2), the web stiffener's sizes (p_3), the edge stiffener's sizes (p_4), the section corners radiuses (p_5), the web stiffener's shapes (p_6 and p_7), the flange stiffener's positions (p_{15}) and the flange stiffener's sizes (p_{16} and p_{17}).

The single parameter response surface is always used for conventional optimization design since it is easily obtained by an orthogonal test. However, it is insufficient for optimization if one does not understand the interaction between parameters.

Figures 6-8 show the double parameters response surface. It is convenient to find the highest buckling and smallest developed stresses in Figure 6; it appears at the web stiffener's locations close to the web flange junctions (p_1 = 1 mm and p_2 = 1 mm).

However, there are 8 response surfaces corresponding to any two of the three parameters (62 response surfaces in total), so it is very challenging to search manually for the maximum buckling and the minimum developed stress values, even when the response surfaces are provided. The ANSYS workbench provides different goal-driven Optimization algorithms that could account for a complex relationship between the channel sections input and the output parameters. A multi-objective genetic algorithm (MOGA) was used to automatically compute the exact parameter values in this study.

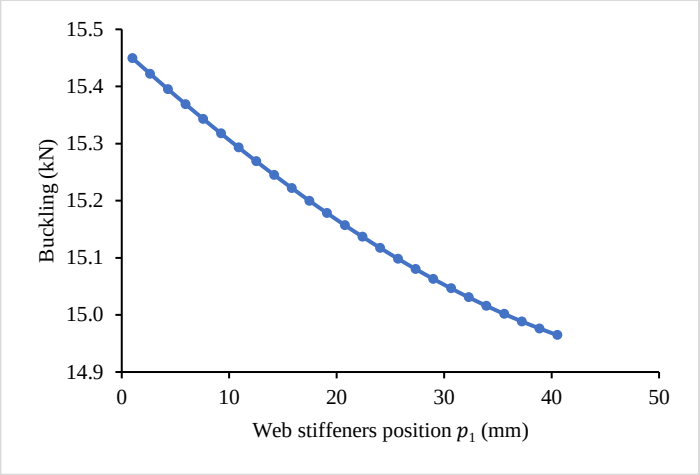

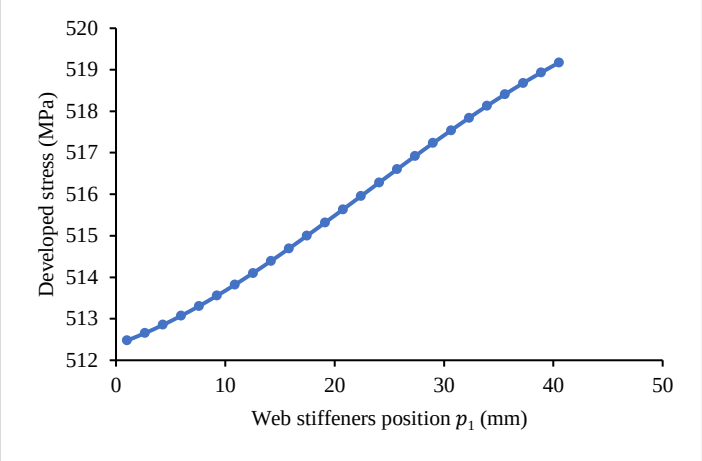

Figure 4: Single parameter response for different positions of web stiffeners p_1 (a) buckling loads and (b) Developed stresses.

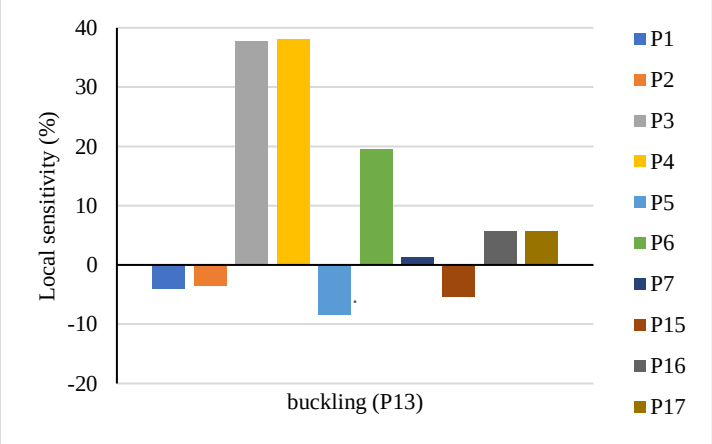

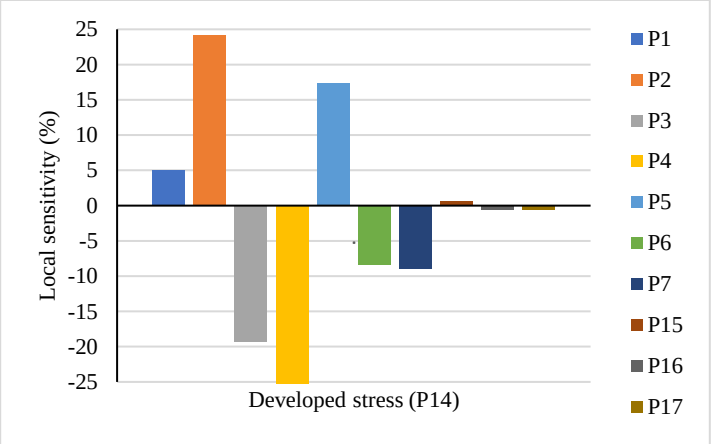

Figure 5: Local sensitivity bar of single parameter.

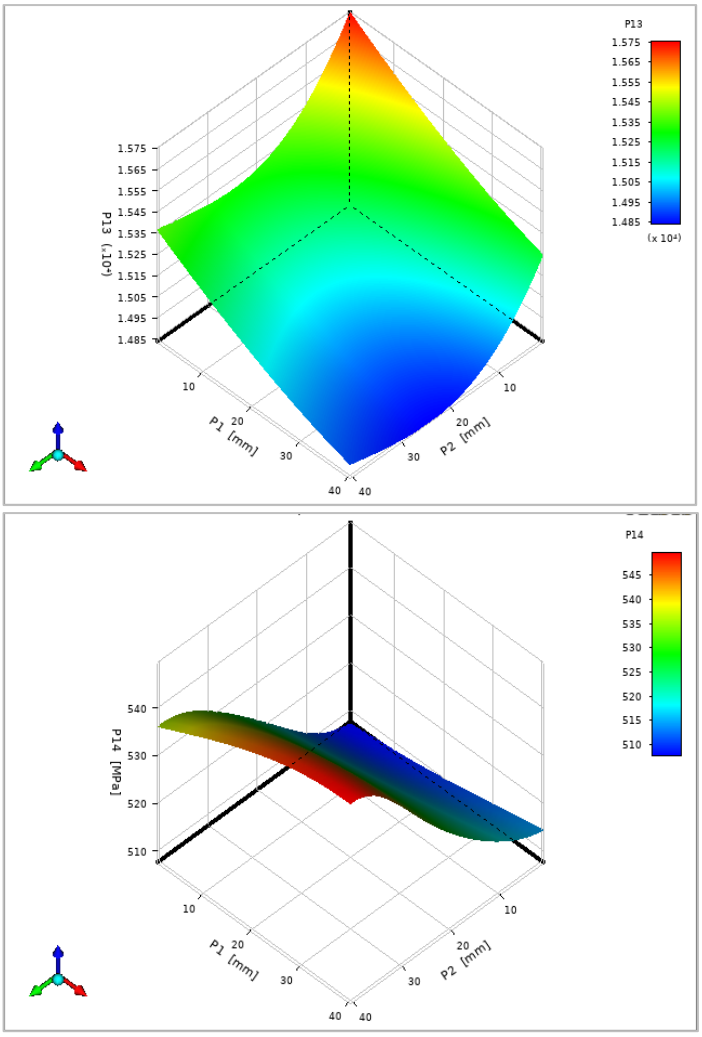

Figure 6: Double parameters response for different positions of web stiffeners p_1 and p_2 (a) buckling and (b) developed stresses.

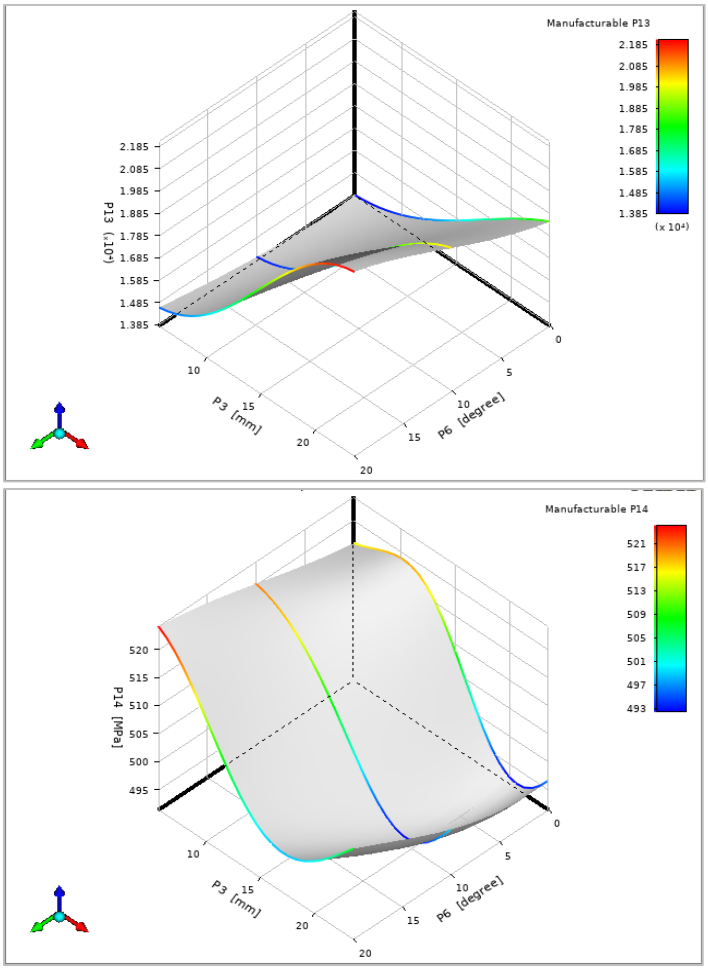

Figure 7: Double parameters response for different sizes of web stiffeners p_3 and p_6 (a) buckling and (b) developed stresses.

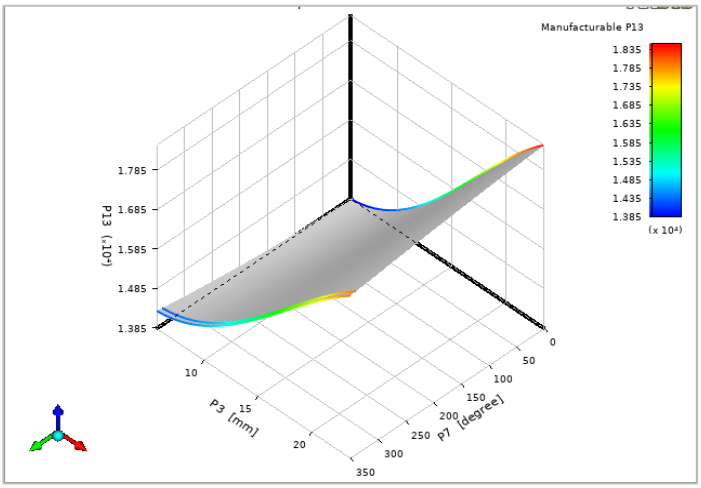

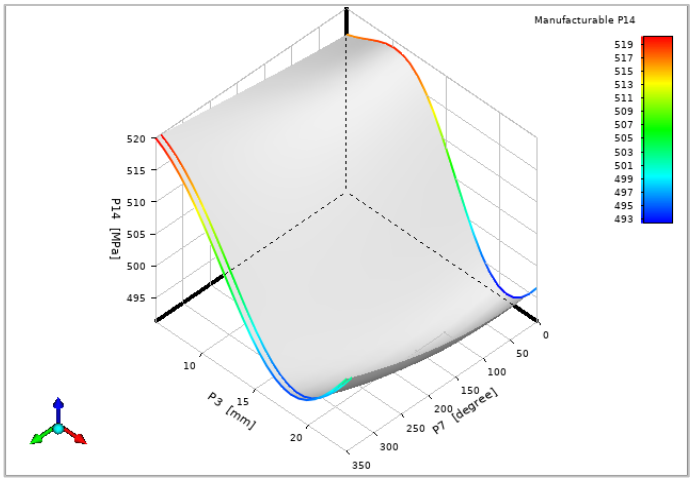

Figure 8: Double parameters response for different sizes of web stiffeners p_3 and p_7 (a) buckling and (b) developed stresses.

4.3 Optimization results

The MOGA method was used to perform Response Surface Optimization. The aim was to obtain optimal design for the channel section that enhanced ultimate bending strength capacity. In the first place, the target objectives were to maximize buckling (p_{13}) and minimize maximum developed stresses (p_{14}) of the channel sections. Several different scenarios were used to determine optimal design candidates. These included minimizing the maximum developed stresses, maximizing buckling, and minimizing the maximum developed stresses and maximizing buckling. Table 1 shows an example of these scenarios, where the 'Goal' was to minimize maximum developed stresses (p_{14}) and maximize buckling (p_{13}). From this, three design candidate points were found which they had almost the same design variables (parameter dimensions). Based on the results of Table 1, the design variables were slightly adjusted to produce a new optimal channel section (i.e. Candidate 6). The design candidate was then loaded up to failure to obtain collapse load-displacement curves as indicated in Figure 9. These processes were repeated to obtain other design candidate point results (i.e. Candidate 1-5).

Table 2 summarizes the buckling and ultimate bending strength of the cross-sectional geometries obtained from the Optimization process (which reference to Figure 1 for the parameters used) and compare them with the standard lipped channel section with the same amount of material and the same section height taken as a starting point. Candidate 1 and 4 were obtained when the 'Goal' was to minimize maximum developed stresses (p_{14}), Candidate 2 and 5 were obtained when the 'Goal' was to maximize buckling (p_{13}), and Candidate 3 and 6 were obtained when the 'Goal' was to minimize maximum developed stresses (p_{14}) and maximize buckling (p_{13}). The resulting cross-sectional

shapes and comparison between flexural strength capacity of the various optimal design candidate points are shown in Figure 9. A number of interesting observations can be made from Figures 9-10 and Tables 1-2:

- The reference channel section provided considerably better buckling compared to the standard lipped channel by 15%, whereas the ultimate moment capacity was noticeably improved by 3%.
- Adding flange stiffeners to the reference section resulted in further enhancement in the buckling and ultimate moment capacity by 16% and 4%, respectively.
- By changing the position, size and shape of web stiffeners, lip width, and section corners' radiuses as well as including the cold work effect at the sections' corners and stiffeners' bends of the reference channel Optimized sections could be obtained (Candidate 1-3) with significantly better buckling. The gains for the candidates of 1, 2 and 3 were 96%, 101% and 100%, respectively, compared to the standard lipped channel. At the same time, the ultimate moment capacity was also improved by 12%, 7% and 12%, respectively.
- Similarly, the optimal design of the channel sections was obtained by changing the position, size and shape of web stiffeners, the position and size of flange stiffeners, lip width, and section corners' radiuses as well as including the cold work effect at the sections' corners and stiffeners' bends of the reference section with having flange stiffeners (Candidate 4-6). The significant increases in buckling for the candidate 4, 5 and 6 were 78%, 98% and 84%, respectively. At the same time, the ultimate moment capacity was also significantly increased by 15%, 8% and 17%, respectively.
- For all design candidates (1-6), the channel section strived to increase its buckling and ultimate moment capacity by (1) decreasing the position of web stiffeners (converged to minimum defined vales of (p_1 = 1.0 mm and p_2 = 1.0 mm) or moving web stiffeners toward the web flange junctions as much as possible), (2) reducing the section corners' radiuses to minimum defined value of (p_5 = 2.9 mm), and (3) increasing the angle between the web stiffeners and the web (p_6 = 15 degree and p_7 = 345 degree). This was due to the combined effect of (1) increasing the sectional modulus, (2) reducing the distortional buckling slenderness, and (3) the cold work effect in the section corners (smaller corner radius has greater strength enhancement). This observation was consistent with previous study [30].
- For design candidate (1-3), while the channel section converged to the same web stiffeners size (p_3 = 19.0 mm), the Optimized sections had different lip widths and flange widths depending on the target objectives (note that the total developed length of the channel section and the section height remain constant). For instance, the section tended to converge at smaller lip and wider flange width (p_3 = 16.0 mm and p_8 = 43.5) when the target was to minimize maximum developed stress in the section (Candidate 1), whereas the section tended to take larger lip and smaller flange width (p_3 = 18.0 mm and p_8 = 41.5) when the target was to maximize buckling (Candidate 2).
- For design candidate (4-6), while the channel section tended to have the same position and size of flange stiffeners (p_{15} = 5.0 mm and p_{16} = p_{17} = 43.5), the sections had various web stiffeners sizes, lip widths, and flange widths based on target objectives. Candidate 4 obtained from minimizing maximum developed stress had web stiffener size, lip width and flange width of 14.4 mm, 13.5 mm, and 28.7 mm, respectively. However, candidate 5 obtained from maximizing buckling had web stiffener size, lip width and flange width of 22.0 mm, 18.0 mm, and 23.0 mm, respectively.
- For all design candidates (1-6), increasing the web stiffener size and lip width up to certain limit significantly improved buckling of the channel section which was effective in suppressing cross-sectional instability, resulting in a significantly increased ultimate moment capacity (as shown in Table 1). At the same time, these cross-sections also exhibited a considerably increased stiffness (as shown in Figure 9), which is a direct result of the stiffeners delaying and mitigating the stiffness degradation due to buckling. It is noted that the increasing stiffeners size was accounting for in the total developed length of the channel section and that, therefore, the flange width of the design candidates is less than that of the reference section. Nevertheless, increasing the stiffeners size beyond certain limit (Candidate 2 and 5) still considerably improved distortional buckling of the channel section, whereas it did not have a significant effect on the ultimate moment capacity and it actually noticeably reduced the ultimate moment capacity in design candidate 2 and 5 compared to 1 and 4 (by 5% and 7%, respectively). This is a result of significant reduction of the sectional modulus in the minor axis which made these cross-sections prone to fail by distortional-global interaction buckling and consequently led to lower ultimate moment capacities for the beam sections. This observation was consistent with previous study [30].
- The optimum shape of the channel section could be obtained when the target objectives were to apply both constrains minimizing maximum developed stress and maximizing buckling in the sections. This led to an optimal design of the channel section (candidate 6) with significantly increasing both stiffness and bending strength and the cold work effects.
- Excluding the cold work effects in the sections' corners and stiffeners' bends had noticeable effect on the ultimate moment capacity of the channel sections (as indicated in Table 1), despite the insignificant effect for standard one, which the cold work effects were included

only in the sections' corners. The maximum percentage of decrease in the ultimate moment capacities without the cold work effect was about 1% to 3%, confirming that both the geometry shape and the cold work effect were very significant.

Table 1: Candidate design when the target objectives were maximizing buckling and minimizing developed stresses (Candidate 6).

Table of Schematic D4: Optimization				
	A	B	C	D
1	Optimization Study			
2	Minimize P14	Goal, Minimize P14 (Higher importance)		
3	Maximize P13	Goal, Maximize P13 (Lower importance)		
4	Optimization Method			
5	MOGA	The MOGA method (Multi-Objective Genetic Algorithm) is a variant of the popular NSGA-II (Non-dominated Sorted Genetic Algorithm-II) based on controlled elitism concepts. It supports multiple objectives and constraints and aims at finding the global optimum.		
6	Configuration	Generate 10000 samples initially, 2600 samples per iteration and find 3 candidates in a maximum of 100 iterations.		
7	Status	Converged after 43214 evaluations.		
8	Candidate Points			
9		Candidate Point 1	Candidate Point 2	Candidate Point 3
10	P1 - Top stiffeners' positions (mm)	1.3749	1.7909	2.0326
11	P2 - Bottom stiffeners' positions (mm)	2.9166	1.1158	1.8162
12	P3 - Stiffeners' tips moved (mm)	16.164	15.523	15.713
13	P4 - Edge stiffeners' widths (mm)	13.563	13.619	13.665
14	P5 - Section corners' radiuses (mm)	2.9318	3.0302	2.9797
15	P6 - Top stiffeners' rotations (degree)	18.392	19.138	16.62
16	P7 - Bottom stiffeners' rotations (degree)	345	340	345
17	P8 - Flange widths (mm)	28.753	29.086	28.721
18	P9 - Commands (APDL) 2 ARG1	571.29	567.15	560.86
19	P10 - Commands (APDL) 2 ARG1	570.38	568.39	572.14
20	P15 - Flange stiffeners' positions (mm)	5.8403	5.3296	5.5855
21	P16 - Top flange stiffeners' sizes (mm)	4.8369	4.4881	4.8684
22	P17 - Bottom flange stiffeners' sizes (mm)	4.7372	4.8222	4.9765
23	P13 - Total Deformation Load Multiplier	★★ 21349	★★ 21283	★★ 20995
24	P14 - Equivalent Stress Maximum (MPa)	★★★ 456.38	★★★ 456.27	★★★ 455.59

Table 2: Buckling and ultimate moment capacity of optimal design for CFS channel sections. M_u, M_{uc} stand for ultimate moment capacity without and with the cold work effect, respectively.

Section type	P13 (kN)	P14 (MPa)	M_u (kNm)	M_{uc} (kNm)	M_{uc}/M_u	$M_{uc}/M_{uc}^{standard}$
Standard (a)	11.7	-	10.34	10.34	1.00	1.00
Reference (b)	13.4	546.5	10.64	10.69	1.01	1.03
Candidate 1	22.9	455.3	11.30	11.58	1.03	1.12
Candidate 2	23.5	484.5	10.94	11.07	1.02	1.07
Candidate 3	23.3	460.0	11.34	11.59	1.03	1.12
Reference (c)	15.3	513.8	10.88	11.12	1.02	1.07
Candidate 4	20.8	455.0	11.60	11.87	1.03	1.15
Candidate 5	23.1	517.0	10.96	11.20	1.03	1.08
Candidate 6	21.5	458.0	11.90	12.09	1.02	1.17

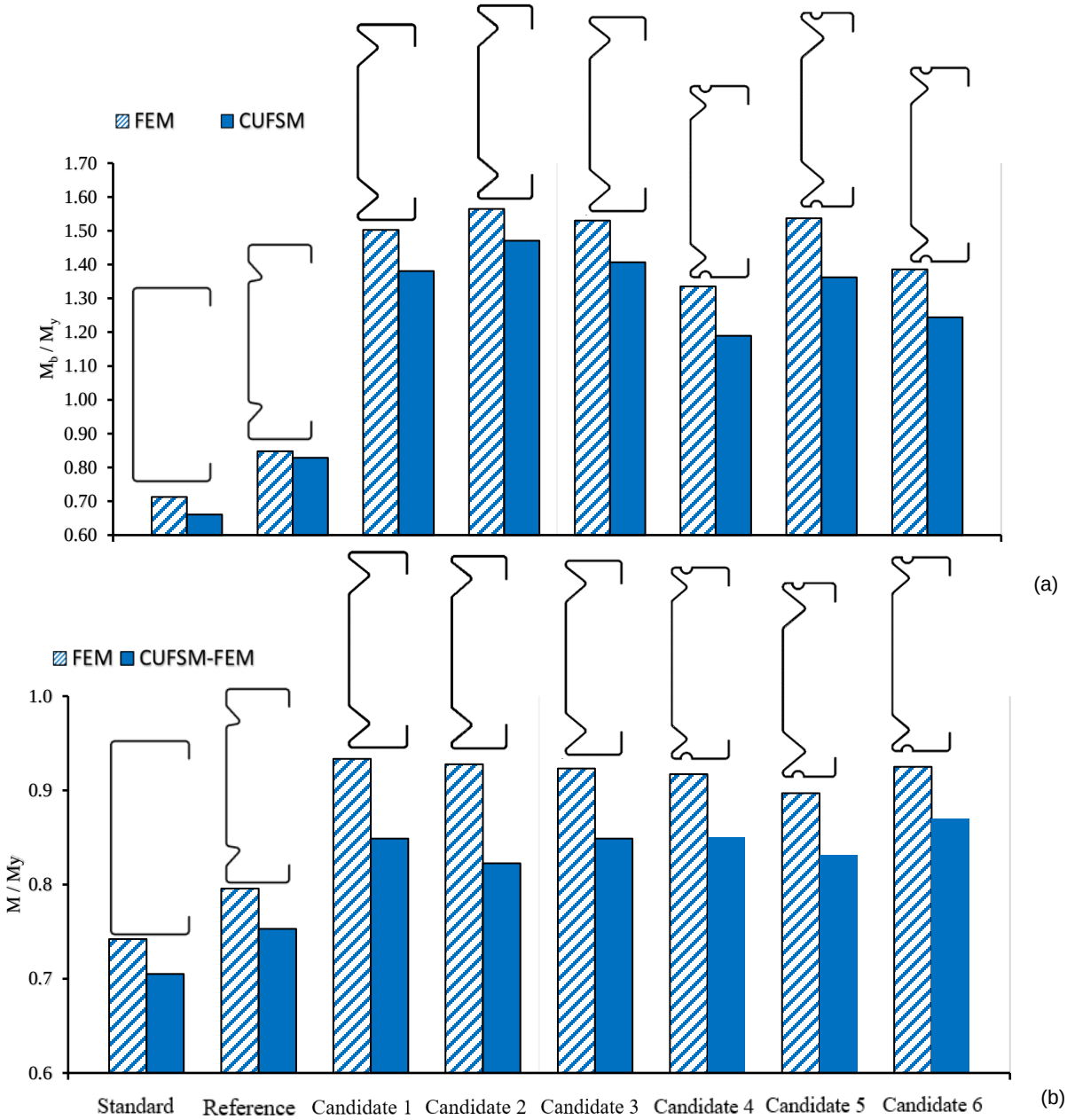

Fig. 9. Flexural strength to yield ratio of the cross sections for (a) buckling and (b) ultimate moment. CUFSM-FEM results obtained by transferring buckling mode shapes from CUFSM to FE models

5. Conclusions

This paper presents a practical method to obtain more efficient cold roll formed steel channel sections in bending using detailed Finite Element (FE) modelling and Response Surface Optimization. The FE models developed to replicate four-point beam bending tests of the channel section were validated first, which included geometrically and materially nonlinear analysis with imperfections and the cold work effects. This validated FE model was then utilized to Optimize the buckling and flexural strength of the channel sections. In the Optimization process, the channel section was parameterized in terms of geometric dimensions, imperfections and material properties using the DOE technique to determine the buckling and flexural strength results of the design points. Response surfaces were generated based on the DOE results to study the influences of the stiffener's properties on the section distortional buckling and flexural strength including its location, shape, size and material properties by the cold work at the section corners and stiffener bends. Optimal design of the channel sections was finally selected using the MOGA method. The

following conclusions could be drawn based on the results of this study:

1) By considering both geometry and the cold work effects in the Optimization process, optimal design of the channel section could be obtained with significant gain in buckling and ultimate bending strength up to 100% and 17%, respectively, compared to the standard lipped channel section using the same amount of material.
2) The optimum position of the web and flange stiffeners found to move toward the web-flange junctions as much as possible during the Optimization process resulted in the Optimized cross-sectional shapes for the channel sections. This was a result of the intermediate stiffeners position both increasing the sectional modulus and decreasing the distortional buckling slenderness, which led to ultimately enhance the distortional buckling and ultimate strength capacities as well as mitigating the post-buckling stiffness degradation of the Optimized channel sections.
3) For the channel sections, the increase of section corners' radius did not result in a more optimal solution. Instead, the entire Optimized sections had smaller section corners' radius. This was partly because when increasing the corners' radius, the distortional buckling slenderness of the section and the strength enhancement of the corners decreased, and consequently the buckling and ultimate bending strength was reduced.
4) Comparison between the design candidates indicated that when increasing the size of intermediate web and flange stiffeners and edge stiffeners, a turning point was reached where increasing the stiffeners size reduced the ultimate moment capacity, while marginally improving the distortional buckling, resulting in sections failed in distortional-global interactive buckling modes.
5) The cold work effect induced from the cold roll manufacturing process was found to be significant in the Optimized channel sections, confirming that it had to be included in the FE models for accurately obtaining enhancement in the ultimate moment capacity of the section. The cold work effect was most significant when the sections are less prone to buckling, especially distortional and global-distortional interactive buckling.
6) It was found that both target objectives constrain, which were maximizing buckling and minimizing maximum developed stress, had to be applied in the optimization analysis in order to obtain the optimal design sections with significantly increasing both stiffness and bending strength and the cold work effects.

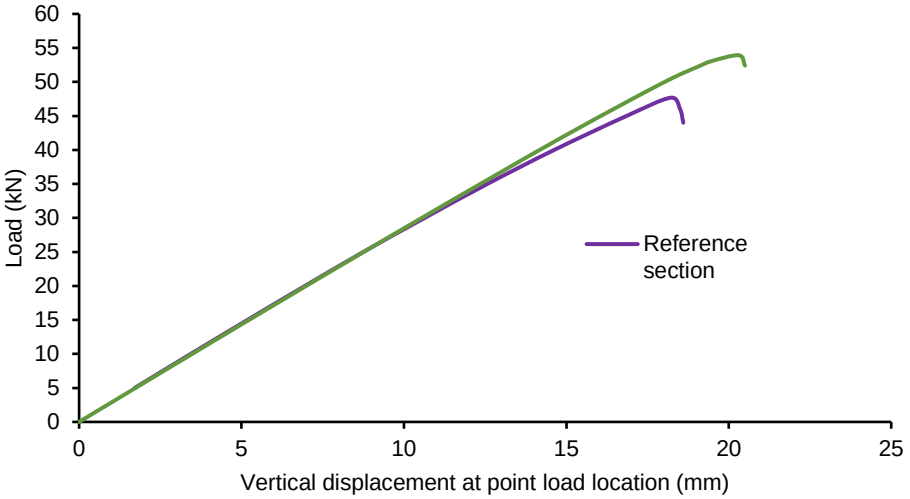

Fig. 10. Load-displacement curves for the channel sections of reference section and design candidate 6 results.

References

[1] AISI. North American specification for the design of cold-formed steel structural members. AISI S100-16. Washington, DC; 2016.

[2] B.S. BSI, Structural use of steelwork in building, Part 5: Code of practice for design of cold formed thin gauge sections, British Standard Institution (1998).

[3] E. CEN, 1-3 Eurocode 3: Design of steel structures-Part 1-3: General rules-Supplementary rules for cold-formed members and sheeting, European Committee for Standardization, Brussels (2006).

[4] K. Magnucki, M. Maćkiewicz, J. Lewiński, Optimal design of a mono-symmetrical open cross section of a cold-formed beam with

cosinusoidally corrugated flanges, Thin-Walled Structures 44(5) (2006) 554-562.

[5] K. Magnucki, P. Paczos, Theoretical shape optimization of cold-formed thin-walled channel beams with drop flanges in pure bending, Journal of constructional steel research 65(8-9) (2009) 1731-1737.

[6] K. Magnucki, M. Rodak, J. Lewiński, Optimization of mono-and anti-symmetrical I-sections of cold-formed thin-walled beams, Thin-Walled Structures 44(8) (2006) 832-836.

[7] M. Ostwald, M. Rodak, Multicriteria optimization of cold-formed thin-walled beams with generalized open shape under different loads, Thin-walled structures 65 (2013) 26-33.

[8] B.P. Gilbert, L.H. Teh, H. Guan, Self-shape optimisation principles: Optimisation of section capacity for thin-walled profiles, Thin-Walled Structures 60 (2012) 194-204.

[9] P. Sharafi, L.H. Teh, M.N. Hadi, Shape optimization of thin-walled steel sections using graph theory and ACO algorithm, Journal of Constructional Steel Research 101 (2014) 331-341.

[10] H. Adeli, A. Karim, Neural network model for optimization of cold-formed steel beams, Journal of Structural Engineering 123(11) (1997) 1535-1543.

[11] J. Lee, S.-M. Kim, H.-S. Park, B.-H. Woo, Optimum design of cold-formed steel channel beams using micro Genetic Algorithm, Engineering Structures 27(1) (2005) 17-24.

[12] J. Lee, S.-M. Kim, H.S. Park, Optimum design of cold-formed steel columns by using micro genetic algorithms, Thin-Walled Structures 44(9) (2006) 952-960.

[13] W. Ma, J. Becque, I. Hajirasouliha, J. Ye, Cross-sectional optimization of cold-formed steel channels to Eurocode 3, Engineering structures 101 (2015) 641-651.

[14] J. Ye, I. Hajirasouliha, J. Becque, A. Eslami, Optimum design of cold-formed steel beams using Particle Swarm Optimisation method, Journal of constructional steel research 122 (2016) 80-93.

[15] J. Ye, I. Hajirasouliha, J. Becque, K. Pilakoutas, Development of more efficient cold-formed steel channel sections in bending, Thin-walled structures 101 (2016) 1-13.

[16] B.P. Gilbert, T.J.-M. Savoyat, L.H. Teh, Self-shape optimisation application: Optimisation of cold-formed steel columns, Thin-walled structures 60 (2012) 173-184.

[17] J. Leng, J.K. Guest, B.W. Schafer, Shape optimization of cold-formed steel columns, Thin-Walled Structures 49(12) (2011) 1492-1503.

[18] H. Liu, T. Igusa, B. Schafer, Knowledge-based global optimization of cold-formed steel columns, Thin-Walled Structures 42(6) (2004) 785-801.

[19] J. Madeira, J. Dias, N. Silvestre, Multiobjective optimization of cold-formed steel columns, Thin-walled structures 96 (2015) 29-38.

[20] M. Moharrami, A. Louhghalam, M. Tootkaboni, Optimal folding of cold formed steel cross sections under compression, Thin-Walled Structures 76 (2014) 145-156.

[21] J.M.S. Franco, J.P. Duarte, E. de Miranda Batista, A. Landesmann, Shape Grammar of steel cold-formed sections based on manufacturing rules, Thin-Walled Structures 79 (2014) 218-232.

[22] J. Leng, Z. Li, J.K. Guest, B.W. Schafer, Shape optimization of cold-formed steel columns with fabrication and geometric end-use constraints, Thin-Walled Structures 85 (2014) 271-290.

[23] B. Wang, B.P. Gilbert, A.M. Molinier, H. Guan, L.H. Teh, Shape optimisation of cold-formed steel columns with manufacturing constraints using the Hough transform, Thin-Walled Structures 106 (2016) 75-92.

[24] Z. Li, J. Leng, J.K. Guest, B.W. Schafer, Two-level optimization for a new family of cold-formed steel lipped channel sections against local and distortional buckling, Thin-Walled Structures 108 (2016) 64-74.

[25] H. Parastesh, I. Hajirasouliha, H. Taji, A.B. Sabbagh, Shape optimization of cold-formed steel beam-columns with practical and manufacturing constraints, Journal of Constructional Steel Research 155 (2019) 249-259.

[26] B. Wang, G.L. Bosco, B.P. Gilbert, H. Guan, L.H. Teh, Unconstrained shape optimisation of singly-symmetric and open cold-formed steel beams and beam-columns, Thin-Walled Structures 104 (2016) 54-61.

[27] B.W. Schafer, The direct strength method of cold-formed steel member design, Journal of constructional steel research 64(7-8) (2008) 766-778.

[28] P. Pan, M. Ohsaki, H. Tagawa, Shape optimization of H-beam flange for maximum plastic energy dissipation, Journal of Structural Engineering 133(8) (2007) 1176-1179.

[29] J. Ye, J. Becque, I. Hajirasouliha, S.M. Mojtabaei, J.B. Lim, Development of optimum cold-formed steel sections for maximum energy dissipation in uniaxial bending, Engineering structures 161 (2018) 55-67.

[30] S. Qadir, V.B. Nguyen, I. Hajirasouliha, B. Cartwright, M. English, Optimal design of cold roll formed steel channel sections under bending considering both geometry and cold work effects, Thin-Walled Structures 157 (2020) 107020.

[31] V.B. Nguyen, C.H. Pham, B. Cartwright, M. English, Design of new cold rolled purlins by experimental testing and Direct Strength Method, Thin-Walled Structures 118 (2017) 105-112.

[32] B. Schafer, T. Peköz, Computational modeling of cold-formed steel: characterizing geometric imperfections and residual stresses, Journal of constructional steel research 47(3) (1998) 193-210.